



NJC

**Nitration of the benzothioxanthene: towards a new class of dyes with versatile photophysical properties**

Journal:	<i>New Journal of Chemistry</i>
Manuscript ID	NJ-ART-11-2019-005804.R1
Article Type:	Paper
Date Submitted by the Author:	06-Dec-2019
Complete List of Authors:	Andres Castan, José María; MOLTECH Anjou Galán, Laura Abad; Curtin University, Curtin Institute for Functional Molecules and Interfaces, School of Molecular and Life Science Li, Shi; university of kentucky dalinot, clément; University of Angers - CNRS, MOLTECH-Anjou Marques, Pablo; University of Angers - CNRS, MOLTECH-Anjou Allain, Magali; University of Angers, Moltech-Anjou UMR CNRS 6200 Risko, Chad; University of Kentucky, Chemistry Monnereau, Cyrille; Ecole Normale Supérieure de Lyon, Laboratoire de Chimie - UMR CNRS 5182 Maury, Olivier; ENS Lyon, dept of chemistry; Blanchard, Philippe; University of Angers - CNRS, MOLTECH-Anjou Cabanetos, Clement; Univ Angers, Moltech;

SCHOLARONE™  
Manuscripts

## PAPER

## Nitration of the benzothioxanthene: towards a new class of dyes with versatile photophysical properties

Received 00th January 20xx,  
Accepted 00th January 20xx

DOI: 10.1039/x0xx00000x

José María Andrés Castán,<sup>a†</sup> Laura Abad Galán,<sup>b†</sup> Shi Li,<sup>c</sup> Clément Dalinot,<sup>a</sup> Pablo Simón Marqués,<sup>a</sup> Magali Allain,<sup>a</sup> Chad Risko,<sup>\*c</sup> Cyrille Monnereau,<sup>b</sup> Olivier Maury,<sup>\*b</sup> Philippe Blanchard,<sup>a</sup> Clément Cabanetos<sup>\*a</sup>

The selective mono-nitration of benzothioxanthene (BTXI) is demonstrated herein. This leap opens doors to a wide range of chemical reactions since the nitro compound was successfully reduced into a primary amine that was, in turn, converted into an azide. Beyond the chemical achievement, this new series of functionalized BTXI was fully characterized, including from a photophysical point of view, expanding the scope of this promising rylene to build a new electroactive  $\pi$ -conjugated platform for electronic organic purposes.

### Introduction

Organic semiconductors have attracted considerable research attention over the last few decades. Consequently, a wide variety of  $\pi$ -conjugated molecular- and macromolecular-based semiconductors have been synthesized and characterized. Among them, imide-containing rylenes hold intrigue as a molecular platform to build robust materials, as they have excellent thermal, chemical, and photochemical stabilities, as well as intriguing electronic and redox properties.<sup>1</sup> As a result, numerous studies have been reported so far and the very large majority of the latter deals with the synthesis, functionalization and use of naphthalene and perylene diimide derivatives. Largely forgotten, *N*-(alkyl)benzothioxanthene-3,4-dicarboximide (BTXI, Figure 1), a sulfur containing rylene-imide dye, has clearly been neglected as there are fewer than a dozen of papers in the literature.<sup>2</sup>

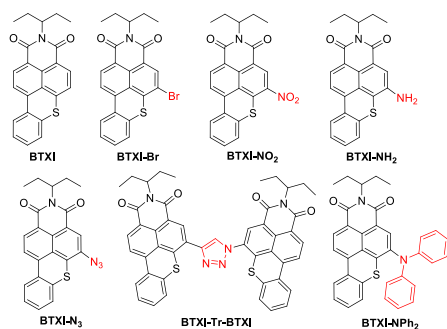


Figure 1. Expansion of BTXI core functionalization

<sup>a</sup> Laboratoire MOLTECH-Anjou, UMR CNRS 6200, UNIV Angers, SFR MATRIX, 2 Bd Lavoisier, 49045 Angers Cedex, France

<sup>b</sup> Univ Lyon, ENS de Lyon, CNRS UMR 5182, Université Claude Bernard Lyon 1, F-69342 Lyon, France.

<sup>c</sup> Department of Chemistry & Center for Applied Energy Research, University of Kentucky, Lexington, KY 40506, USA.

<sup>†</sup> These authors contributed equally.

Electronic Supplementary Information (ESI) available: [details of any supplementary information available should be included here]. See DOI: 10.1039/x0xx00000x

Solely functionalized on the nitrogen atom of the imide group, we recently reported the selective mono-bromination of the BTXI core (BTXI-Br, Figure 1) opening doors to the design of new  $\pi$ -conjugated molecules for organic electronic applications.<sup>3</sup> In this context and considering the high potential of this building block, efforts are currently devoted to further functionalize the BTXI with other functional groups than halogen atoms to explore complementary chemical reactions to conventional palladium-catalyzed cross couplings. In this context, we report herein an efficient approach to afford a new nitro derivative, a key precursor to amino BTXI that can be further involved in conventional and modified Sandmeyer reactions, thus widening the scope of design principles.

### Results and discussion

First, one molar equivalent of fuming nitric acid was added to a solution of BTXI at room temperature, leading to the formation of a new and predominant species. However, and regardless of the reaction time, the full conversion of the starting BTXI can only be achieved with an excess of nitric acid, *i.e.*, two molar equivalents (Figure 2).

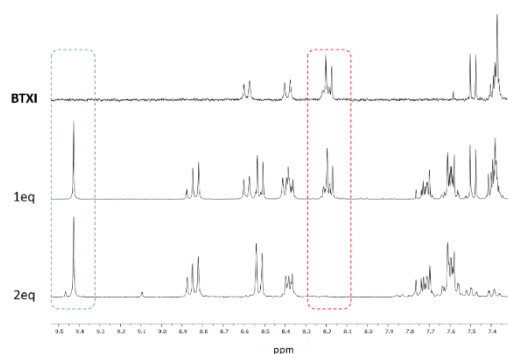


Figure 2. NMR spectra of the reaction mixtures depending on the number of molar equivalent of nitric acid added at room temperature

PAPER

New Journal of Chemistry

Upon purification, integration of the signals revealed the presence of 11 aliphatic protons, attributed to the ethylpropyl side chain, and 7 in the 7.5 to 9.5 ppm range, thus confirming the selective and single substitution of the aromatic core (Figure S1-B). The nature of the substituent was thereafter confirmed by high-resolution mass spectrometry (see SI for details). Nonetheless, exact position of the nitro group remained to be solved.

Density functional theory (DFT) calculations were performed at the OT- $\omega$ B97X-D/6-31g(d,p) level of theory to determine the low-energy nitro-substitution site for each unique and potential **BTXI-NO<sub>2</sub>** derivative. Determination of the relative free energies ( $\Delta G^\circ$ ) of the potential mono-nitro products (Figure 3 and Table S2) reveals that NO<sub>2</sub> has a thermodynamic preference for the position labelled 4 but with positions 5, 6, and 7 being relatively close in energy.

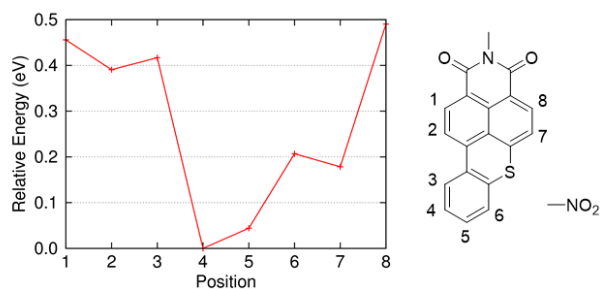
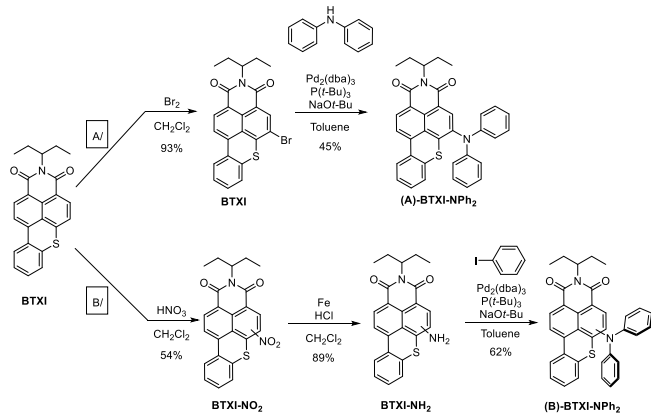


Figure 3. Relative energies of **BTXI-NO<sub>2</sub>** derivatives calculated at the OT- $\omega$ B97XD/6-31G(d, p) level of theory. NB: the alkyl group was truncated to a methyl to reduce the computational cost.

Faced with the difficulty of crystal growth, the molecular structure of **BTXI-NO<sub>2</sub>** was experimentally investigated by nuclear overhauser effect spectroscopy (NOESY). In contrast with the theoretical predictions, it turned out that the nitration occurred on the naphthyl ring and more precisely either on position 8 or 7, *i.e.*, as for **BTXI-Br** (Figure S2).

To support this inference, an indirect synthetic strategy was subsequently considered, consisting of the preparation and comparison of two structural isomers obtained either from the structurally well solved **BTXI-Br** (Scheme 1, approach A) or from the nitro derivative (Scheme 1, approach B).

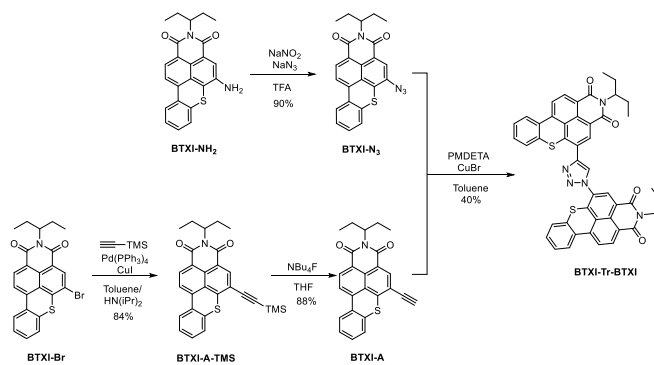


Scheme 1. Two synthetic routes towards **BTXI-NPh<sub>2</sub>** from **BTXI-Br** (A) and **BTXI-NO<sub>2</sub>** (B).

Once isolated and purified by column chromatography, both molecules were analyzed by NMR revealing a perfect superimposition of their proton spectra, suggesting a similar grafting position (Figure S3). The latter was subsequently confirmed by X-ray diffraction since single crystals of **(B)-BTXI-NPh<sub>2</sub>** were successfully grown and analyzed (Figure S31).

Hence, while computational chemistry predicted a functionalization in position 4, corresponding to the thermodynamic product (Figure 2), the nitration conditions reported here result with the exclusive formation of the kinetic product. This nitro derivative opens doors to a wide range of chemical reactions and possible designs for novel  $\pi$ -conjugated chromophores. For instance, the latter was successfully reduced

into a primary amine (**BTXI-NH<sub>2</sub>**) that was, in turn, converted into an azide, thus affording the “clickable” **BTXI-N<sub>3</sub>** (Scheme 2). Besides palladium-catalyzed cross coupling reactions, the copper-catalyzed azide-alkyne cycloaddition (CuAAC) is a major tool in synthetic chemical strategies spanning various applications from drug discovery to materials science. As a proof of concept, the **BTXI-Tr-BTXI** dimer was synthesized by combining both coupling approaches (Scheme 2) since the alkyne derivative (**BTXI-A**) was prepared from the bromo derivative *via* Sonogashira cross-coupling reaction.



Scheme 2. Synthesis and use of the azido derivative **BTXI-N<sub>3</sub>**.

Though isolated with a modest yield, mainly due to the lack of solubility of the target compound, the dimer demonstrates the potential, reactivity and complementarity of both coupling methods to expand the scope of  $\pi$ -functional **BTXI**-based materials.

Considering that rylene derivatives are usually characterized by distinctive photophysical properties and the almost total absence of data related to the **BTXI**,<sup>4</sup> the spectroscopic features of the series reported herein were naturally investigated. In addition to absorption and emission profiles, fluorescence lifetimes ( $\tau_{\text{obs}}$ ) and quantum yields ( $\Phi_f$ ) were determined in dichloromethane solutions (Table 1). Due to the presence of heavy heteroatoms (S and in one instance Br) that are expected to increase spin-orbit coupling (SOC) within the molecule,<sup>5</sup> the potential of these derivatives to generate singlet oxygen ( $\Phi_\Delta$ ) based on their triplet excited states, was also quantified.<sup>6</sup> The absorption and emission spectra of all the molecules are displayed in Figure 4.

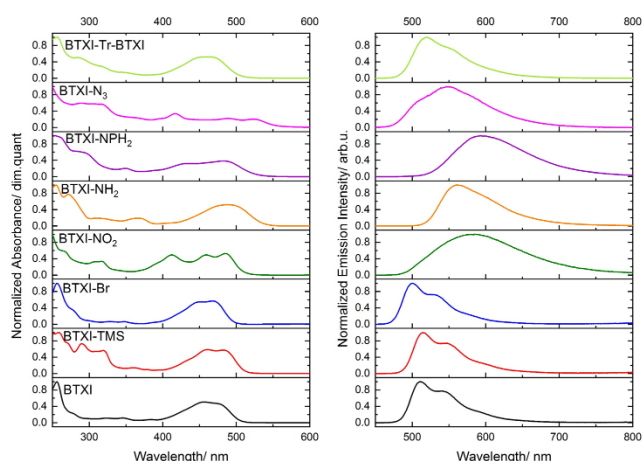


Figure 4. Normalized absorbance (a) and emission (b) of all **BTXI** derivatives in diluted dichloromethane solutions at room temperature.

Except for **BTXI-NH<sub>2</sub>** and, in a somewhat lesser degree, **BTXI-NPh<sub>2</sub>**, all studied derivatives are characterized by structured spectra both in absorption and in emission. For **BTXI**, **BTXI-Br**, **BTXI-N<sub>3</sub>** and **BTXI-Tr-BTXI**, the main transition located at *ca* 480 nm can thus be assigned to a localized  $\pi$ - $\pi^*$  transition of the polyaromatic **BTXI** core, whose position is slightly affected by the presence of substituents. Time-dependent DFT (TDDFT) calculations at the OT- $\omega$ B97X-D/6-31g(d,p) level of theory confirm this assignment, also showing a significant red-shift for **BTXI-NH<sub>2</sub>** when compared to other **BTXI** derivatives (Figure S19). As expected for such transitions, no significant solvatochromism was observed for the emission band of **BTXI** when moving from toluene to *N,N*-dimethylformamide (DMF) (Figure S4). In stark contrast, **BTXI-NH<sub>2</sub>** shows broad and structureless absorption and emission bands which are i) significantly red-shifted compared to other **BTXI** derivatives (*ca* 490 nm) and ii) solvent dependent (Figure S5).

Plotting the energy of the Stokes shift against the solvent polarizability following the Lippert-Mataga equation gave a clear linear tendency with positive slope (Figure S6). All these features are consistent with an assignment of this band to a charge transfer (CT) transition, indicative of push pull effect between the amino and naphthalimide parts of the molecule. Similar features in the absorption and emission spectra were found for **BTXI-NPh<sub>2</sub>**. In the latter case, the bathochromic shift of the emission compared to **BTXI-NH<sub>2</sub>** (Figure S7) can be rationalized on the basis of a stronger reorganization between a distorted ground state (induced by the steric hindrances of the phenyl substituents) and a more planar excited state. For **BTXI-NPh<sub>2</sub>**, natural transition orbitals (NTOs) derived from the TDDFT calculations reveals that the transitions with significant oscillator strength are mainly between the amino and naphthalimide moieties, confirming the CT-like assignment (Figure S25).

Comparatively with the other **BTXI** derivatives, **BTXI-NO<sub>2</sub>** exhibits a red-shifted broad and structureless emission band

alongside **BTXI-NH<sub>2</sub>**. However, it is noteworthy that this band does not display a solvatochromic behaviour and therefore cannot clearly be assigned to a CT (Figure S8). Furthermore, a clear contribution of phosphorescence from the triplet state band at 650 nm could be observed from the emission spectrum of **BTXI-NO<sub>2</sub>** when recorded at 77K in a 1:4 mixture of MeOH and EtOH. Then, by applying a delay of 0.05 ms, the phosphorescence band could be observed (Figure S9) and an energy at zero-phonon transition of 15,870  $\text{cm}^{-1}$  was recorded. Quite counterintuitively, while a phosphorescence band is also present in **BTXI-Br**, in which the heavy bromine substituent is expected to significantly enhance SOC, and thus facilitates the spin forbidden S1-T1 intersystem crossing (Figure S11), its magnitude turns out to be much lower than that of **BTXI-NO<sub>2</sub>**, witnessing a faster intersystem crossing. Regarding **BTXI-NPh<sub>2</sub>** and **BTXI-Tr-BTXI** the phosphorescence band was also observed probably due to distortions of the  $\pi$ -conjugated backbone, inducing an enhancement of SOC since triplet state energy of 14,600 and 15,385  $\text{cm}^{-1}$  were calculated respectively. On the other hand, 77K measurements performed on all other **BTXI** derivatives of the series did not show any significant triplet emission (Figures S12-S17).

The fluorescence quantum yields were determined for all molecules and turned out to be strongly dependent on the nature of the substituents. While **BTXI** and **BTXI-TMS** present almost quantitative quantum yields, the addition of Br, NH<sub>2</sub>, NO<sub>2</sub>, NPh<sub>2</sub>, N<sub>3</sub> or Tr-BTXI indeed seems to efficiently quench their emission (Table 1). In the case of **BTXI-NH<sub>2</sub>** and **BTXI-NPh<sub>2</sub>**, the CT character could explain the difference in  $\Phi_f$ , as the distinctively lower recorded emission energy is prone to induce more efficient non-radiative deactivation through vibronic coupling between the ground and excited electronic states (energy gap law). Regarding **BTXI-N<sub>3</sub>**, a non-radiative decay through photoinduced electron transfer (PET) between **BTXI** core and azido substituent would presumably be the most efficient pathway of quenching, as previously reported in the literature for similar compounds.<sup>7</sup>

For **BTXI-Br**, the presence of a bromine atom might enhance intersystem crossings (ISC) and therefore quenches emission from singlet state, while providing the aforementioned triplet emission. With regard to **BTXI-NO<sub>2</sub>**, the presence of a long-lived triplet state even at room temperature can be related to its low fluorescence quantum yield, thus confirming the very efficient SOC and thus ISC achieved upon nitro substitution. This was further confirmed by the fact that **BTXI-Br** and **BTXI-NO<sub>2</sub>** displayed significant singlet oxygen generation efficiencies of 0.11 and 0.42, respectively. Although the large magnitude of ISC in **BTXI-NO<sub>2</sub>** is quite surprising, the occurrence of such effects in nitro substituted polyaromatics is well documented in literature.<sup>5c,8</sup> In addition to a lowest lying emitting  $^3\pi$ - $\pi^*$  state, this feature is attributed to the existence of a more energetic  $^3n$ - $\pi^*$  state centred on the nitroaromatic part of the molecule. The latter state, being comparatively closer in energy to the  $^1\pi$ - $\pi^*$  state, and involving a change in electronic configuration ( $^1\pi$ - $\pi^* \rightarrow ^3n$ - $\pi^*$ ), favours important SOC effects, and is at the origin of the outstanding properties of **BTXI-NO<sub>2</sub>**. Finally, the **BTXI-Tr-BTXI** dimer presents a lower quantum yield in comparison to a

single **BTXI** and shows relatively high generation of singlet oxygen, which may also be enhanced by the previously mentioned conformation restrictions that give rise to  $\pi$ -distorted ground state geometry.<sup>7</sup> A similar observation and

conclusion can be drawn for **BTXI-NPh<sub>2</sub>**, which shows the strongest singlet oxygen generation within the series witnessing important SOC despite of the absence of heavy atoms.

	$\lambda_{\text{abs}}(\text{max})$ (nm)	$\lambda_{\text{em}}$ (nm)	Stokes Shift ( $\text{cm}^{-1}$ )	$\Phi_{\text{F}}^{\text{a}}$	$\tau_{\text{obs}}$ (ns)	$\Phi_{\Delta}^{\text{b}}$	$E_{\text{Triplet}} (\text{cm}^{-1})^{\text{c}}$
<b>BTXI</b>	455	510	2,370	0.99	7.48	0.00	-
<b>BTXI-TMS</b>	461	515	2,275	0.86	8.55	0.00	-
<b>BTXI-Br</b>	469	500	1,322	0.78	6.49	0.11	14,925
<b>BTXI-NO<sub>2</sub></b>	486	585	3,482	0.01	8.14	0.42	15,870
<b>BTXI-NH<sub>2</sub></b>	490	555	2,390	0.67	11.17	0.00	-
<b>BTXI-NPh<sub>2</sub></b>	483	600	4,037	0.33	10.68	0.46	14,600
<b>BTXI-N<sub>3</sub></b>	523	550	939	0.11	5.84	0.00	-
<b>BTXI-Tr-BTXI</b>	458	520	2,603	0.56	6.91	0.23	15,385

<sup>a</sup> Measured using coumarine-153 as reference ( $\Phi_{\text{F}} = 0.45$  in MeOH); <sup>b</sup> Measured using phenalene as reference ( $\Phi_{\text{F}} = 0.95$  in DCM).<sup>12</sup> <sup>c</sup> Calculated at the first band maximum.

Table 1. Photophysical data of the BTXI derivatives in diluted dichloromethane solution

## Conclusions

Forgotten by the community, we have recently pointed out the potential of the benzothioxanthene block for organic electronic applications. In addition to the previous demonstration of its bromination, opening doors to conventional palladium cross-coupling reactions, we report here the selective mono-nitration of the **BTXI** core. Once fully characterized, this new compound was successfully reduced into an amino derivative that was, in turn, converted in an azido group. **BTXI-N<sub>3</sub>** was found to be perfectly compatible with the well-known, copper-catalyzed azide-alkyne cycloaddition (CuAAC), and this manuscript adds another important string to the bow of the **BTXI** functionalization, design principle and therefore potential applications. Moreover, to gain further insights into the new **BTXI** derivatives reported here, their photophysical properties have been investigated in parallel. While the unsubstituted **BTXI** core presents very high emission efficiency associated with a localized electronic transition, introduction of electron withdrawing or donating substituents on the naphthalene ring strongly modifies the spectroscopic signatures. Moreover, it was demonstrated that large SOC, and thus efficient singlet oxygen generation properties can also be efficiently achieved, not only by classical addition of heavy atom substituents, but also upon the choice of substituents that lead to a ground state distortion of the  $\pi$ -conjugated backbone. For instance, **BTXI-NPh<sub>2</sub>** efficiently combines both marked CT character (red-shifted luminescence with a relevant emission quantum yield) and a large singlet oxygen generation efficiency, making it a potential candidate for application in biophotonics and theranostics.<sup>9</sup>

## Experimental

### General

All reagents and chemicals from commercial sources were used without further purification. Solvents were dried and purified using

standard techniques. Flash chromatography was performed with analytical-grade solvents using Aldrich silica gel (technical grade, pore size 60 Å, 230-400 mesh particle size). Flexible plates ALUGRAM® Xtra SIL G UV254 from MACHEREY-NAGEL were used for TLC. Compounds were detected by UV irradiation (Bioblock Scientific). NMR spectra were recorded with a Bruker AVANCE III 300 (1H, 300 MHz and 13C, 75MHz) or a Bruker AVANCE DRX500 (1H, 500 MHz; 13C, 125 MHz). Chemical shifts are given in ppm relative to TMS and coupling constants J in Hz. IR spectra were recorded on a Bruker spectrometer Vertex 70 and UV-vis spectra with a Perkin Elmer 950 spectrometer. Matrix Assisted Laser Desorption/Ionization was performed on MALDI-TOF MS BIFLEX III Bruker Daltonics spectrometer using dithranol as matrix. High resolution mass spectrometry (HRMS) was performed with a JEOL JMS-700 B/E. Melting points are uncorrected.

### Synthetic procedures

**BTXI-NO<sub>2</sub>**: HNO<sub>3</sub> (0.13 mmol or 0.26 mmol,) solubilized in CH<sub>2</sub>Cl<sub>2</sub> (2 mL) was added dropwise on a stirred solution of **BTXI** (50.0 mg, 0.13 mmol) in CH<sub>2</sub>Cl<sub>2</sub> (3 mL). After 20 minutes, water was added to the reaction mixture and the organic phase was concentrated under vacuum. To get rid of impurities the resulting powder was recrystallized from CH<sub>2</sub>Cl<sub>2</sub> yielding **BTXI-NO<sub>2</sub>** as an orange solid (30.2 mg, 54%). m.p.: 290 - 292 °C. <sup>1</sup>H NMR (500 MHz, CDCl<sub>3</sub>):  $\delta$  (ppm) 9.43 (s, 1H), 8.84 (d,  $J = 8.3$  Hz, 1H), 8.53 (d,  $J = 8.4$  Hz, 1H), 8.42 - 8.36 (m, 1H), 7.74 - 7.69 (m, 1H), 7.63 - 7.56 (m, 2H), 5.10 - 5.01 (m, 1H), 2.31 - 2.19 (m, 2H), 1.99 - 1.88 (m, 2H), 0.91 (t,  $J = 7.5$  Hz, 6H). <sup>13</sup>C NMR (125 MHz, CDCl<sub>3</sub>):  $\delta$  (ppm) 141.5, 139.0, 138.1, 131.7, 131.6, 130.7, 129.2, 127.4, 127.2, 126.2, 125.8, 121.2, 58.1, 25.0, 11.5. HRMS (EI):  $m/z$  calcd for C<sub>23</sub>H<sub>18</sub>N<sub>2</sub>O<sub>4</sub>S: 418.0982, found: 418.0986 ( $\Delta = 1.0$  ppm).

**BTXI-NH<sub>2</sub>**: THF (60 mL) was added to a solid mixture of **BTXI-NO<sub>2</sub>** (500.0 mg, 1.20 mmol) and powdered iron (467.0 mg, 8.40 mmol). Hydrochloric acid (5.00 mL, 37%) was subsequently added and the mixture was heated at 65 °C for 40 minutes. Water was added to quench the reaction and the obtained solid was filtered and washed thoroughly with water. The crude was passed through a pad of neutral alumina (eluent: chloroform) affording **BTXI-NH<sub>2</sub>** (411 mg, 89%) as a red powder. m.p.: 288 - 290 °C. <sup>1</sup>H NMR (300 MHz, CDCl<sub>3</sub>):  $\delta$  (ppm) 8.41 (d,  $J = 8.0$  Hz, 1H), 8.22 - 8.09 (m, 2H), 8.05 (s, 1H), 7.48

– 7.34 (m, 3H), 5.12 – 4.98 (m, 1H), 4.04 (s, 2H), 2.43 – 2.11 (m, 2H), 2.02 – 1.78 (m, 2H), 0.89 (t,  $J = 7.5$  Hz, 6H).  $^{13}\text{C}$  NMR (125 MHz,  $\text{CDCl}_3$ ):  $\delta$  (ppm) 137.3, 134.8, 130.4, 129.7, 128.7, 127.9, 127.3, 126.8, 126.2, 125.3, 119.8, 57.5, 25.1, 11.5. HRMS (FAB):  $m/z$  calcd for  $\text{C}_{23}\text{H}_{20}\text{N}_2\text{O}_2\text{S}$ : 388.1240, found: 388.1250 ( $\Delta = 2.6$  ppm).

**(A)-BTXI-NPh<sub>2</sub>**: Sodium *tert*-butoxyde (26.5 mg, 0.28 mmol),  $\text{Pd}_2(\text{dba})_3$  (10.1 mg, 0.011 mmol), diphenylamine (39.3 mg, 0.23 mmol) and **BTXI-Br** (100.0 mg, 0.22 mmol) were dissolved in dry and degassed toluene (5 mL). Then, a solution of tri-*tert*-butylphosphine in toluene (220  $\mu\text{L}$ , 0.22 mmol) was added and the mixture was heated to reflux and stirred overnight. The reaction was filtered through a silica plug and eluted with ethyl acetate. The solution was concentrated under reduced pressure and the final product was purified by column chromatography on silica gel (eluent:  $\text{CH}_2\text{Cl}_2/\text{Petroleum ether 7:3}$ ) affording an orange solid (53.2 mg, 45%).

**(B)-BTXI-NPh<sub>2</sub>**: Sodium *tert*-butoxyde (35.6 mg, 0.37 mmol),  $\text{Pd}_2(\text{dba})_3$  (14.1 mg, 0.015 mmol), and **BTXI-NH<sub>2</sub>** (60.0 mg, 0.15 mmol) were dissolved in dry and degassed toluene (2.5 mL). Iodobenzene (87  $\mu\text{L}$ , 0.77 mmol) and a solution of tri-*tert*-butylphosphine in toluene (310  $\mu\text{L}$ , 0.31 mmol) were added to the reaction mixture. The latter was heated to reflux and stirred overnight. Once cooled to room temperature, the reaction was filtered through a silica plug ( $\text{CH}_2\text{Cl}_2$ ). The solution was concentrated under reduced pressure and the final product was purified by column chromatography on silica gel (eluent:  $\text{CH}_2\text{Cl}_2/\text{Petroleum ether 7:3}$ ) affording an orange solid (52.0 mg, 62%).

m.p.: 245 – 247 °C.  $^1\text{H}$  NMR (300 MHz,  $\text{CD}_2\text{Cl}_2$ ):  $\delta$  (ppm) 8.59 (d,  $J = 8.2$  Hz, 1H), 8.33 (s, 1H), 8.31 – 8.22 (m, 2H), 7.43 – 7.32 (m, 3H), 7.31 – 7.23 (m, 4H), 7.11 – 7.01 (m, 6H), 5.07 – 4.93 (m, 1H), 2.31 – 2.12 (m, 2H), 1.94 – 1.76 (m, 2H), 0.88 (t,  $J = 7.5$  Hz, 6H).  $^{13}\text{C}$  NMR (75 MHz,  $\text{CD}_2\text{Cl}_2$ ):  $\delta$  (ppm) 146.1, 139.9, 137.6, 136.8, 132.5, 130.3, 129.9, 129.5, 128.2, 128.1, 127.8, 127.5, 126.4, 123.6, 122.3, 120.1, 57.8, 25.4, 11.7. HRMS (EI):  $m/z$  calcd for  $\text{C}_{35}\text{H}_{28}\text{N}_2\text{O}_2\text{S}$ : 540.1866, found: 540.1864 ( $\Delta = 0.4$  ppm).

**BTXI-N<sub>3</sub>**: **BTXI-NH<sub>2</sub>** (50.0 mg, 0.13 mmol) was dissolved in trifluoroacetic acid (0.5 mL) at 0 °C before adding a solution of  $\text{NaNO}_2$  (11.5 mg, 0.17 mmol) solubilized in water (0.1 mL). After 20 min,  $\text{NaN}_3$  (10.9 mg, 0.17 mmol), also solubilized in water (0.1 mL) was added to the reaction mixture. Still stirred for an extra hour at 0 °C, the mixture was warmed up to rt and water was added to quench the reaction. The resulting solid was filtered off, washed thoroughly with water and dried, yielding **BTXI-N<sub>3</sub>** (48.0 mg, 90%). m.p.: 146 – 148 °C (d).  $^1\text{H}$  NMR (300 MHz,  $\text{CDCl}_3$ ):  $\delta$  (ppm) 8.55 (d,  $J = 8.3$  Hz, 1H), 8.37 (s, 1H), 8.27 – 8.18 (m, 2H), 7.48 – 7.39 (m, 3H), 5.19 – 4.95 (m, 1H), 2.41 – 2.14 (m, 2H), 1.98 – 1.80 (m, 2H), 0.90 (t,  $J = 7.5$  Hz, 6H).  $^{13}\text{C}$  NMR was not recorded due to stability issues in solution. IR (neat):  $\text{cm}^{-1}$  2112 ( $-\text{N}_3$ ). MS (MALDI):  $m/z$  calcd for  $\text{C}_{23}\text{H}_{18}\text{N}_4\text{O}_2\text{S}$ : 414.48, found: 305 [ $\text{M}-\text{H}-\text{N}_2$ ] $^+$ .

**BTXI-A**:  $\text{NBu}_4\text{F}$  1M in THF (0.19 mL, 0.19 mmol) was added dropwise to a solution of **BTXI-A-TMS** in anhydrous THF (12 mL). After 1h, water was added to quench the reaction and the organic phase was extracted with dichloromethane, dried with  $\text{MgSO}_4$  and concentrated under reduced pressure. The crude was purified by column chromatography on silica gel (eluent:  $\text{CH}_2\text{Cl}_2$ ) yielding **BTXI-A** (67.0 mg, 88%) as an orange powder. m.p.: 224 – 226 °C (d).  $^1\text{H}$  NMR (300 MHz,  $\text{CDCl}_3$ ):  $\delta$  (ppm) 8.62 – 8.46 (m, 2H), 8.26 – 8.13 (m, 2H), 7.48 – 7.36 (m, 3H), 5.10 – 4.98 (m, 1H), 3.80 – 3.76 (m, 1H), 2.33 – 2.16 (m, 2H), 1.99 – 1.83 (m, 2H), 0.90 (t,  $J = 7.4$  Hz, 6H).  $^{13}\text{C}$  NMR (75 MHz,  $\text{CDCl}_3$ ):  $\delta$  (ppm) 143.6, 136.3, 134.5, 132.8, 131.6, 130.1, 129.9,

128.0, 127.6, 126.9, 126.0, 125.4, 121.6, 119.8, 118.1, 113.3, 87.6, 87.6, 79.6, 57.6, 25.0, 11.5. HRMS (FAB):  $m/z$  calcd for  $\text{C}_{25}\text{H}_{19}\text{NO}_2\text{S}$ : 397.1131, found: 397.1136 ( $\Delta = 1.3$  ppm).

**BTXI-Tr-BTXI**: A solution of 10 drops of *N,N,N',N',N''*-pentamethyldiethylenetriamine (PMDETA) in toluene (45 mL) was degassed five times via freeze-pump-thaw cycling. This solution was then transferred into a Schlenk flask containing **BTXI-A** (38 mg, 0.096 mmol),  $\text{CuBr}$  (12 mg) and **BTXI-N<sub>3</sub>** (36 mg, 0.087 mmol) under argon atmosphere at rt. The reaction mixture was protected from light and stirred overnight. The solvent was removed in vacuo and the residue was purified by chromatography on silica gel (eluent:  $\text{CHCl}_3/\text{MeOH}$  from 100:0 v/v to 99:1 v/v). The resulting solid was dissolved in  $\text{CH}_2\text{Cl}_2$  and then precipitated with pentane affording an orange powder (28 mg, 40%). m.p.: 246 – 248 °C (d).  $^1\text{H}$  NMR (300 MHz,  $\text{CDCl}_3$ ):  $\delta$  (ppm) 9.02 (s, 1H), 8.76 (d,  $J = 7.9$  Hz, 1H), 8.68 (d,  $J = 8.1$  Hz, 1H), 8.62 (s, 1H), 8.48 (s, 1H), 8.40 (d,  $J = 8.2$  Hz, 1H), 8.36 – 8.24 (m, 3H), 7.53 – 7.39 (m, 6H), 5.15 – 5.04 (m, 2H), 2.36 – 2.21 (m, 4H), 2.02 – 1.89 (m, 4H), 0.93 (t,  $J = 7.4$  Hz, 12H).  $^{13}\text{C}$  NMR (125 MHz,  $\text{CDCl}_3$ ):  $\delta$  (ppm) 130.6, 130.1, 128.6, 128.1, 127.5, 124.2, 121.9, 120.7, 120.2, 29.9, 25.1, 25.0, 11.5, 11.5. HRMS (FAB):  $m/z$  calcd for  $\text{C}_{48}\text{H}_{38}\text{N}_5\text{O}_4\text{S}_2$ : 812.2360, found: 812.2364 [ $\text{M}+\text{H}$ ] $^+$  ( $\Delta = 0.5$  ppm).

## Conflicts of interest

There are no conflicts to declare.

## Acknowledgements

Authors thank the MATRIX SFR of the University of Angers. J.M.A.C. and P.S.M. thanks the European Union's Horizon 2020 research and innovation program under Marie Skłodowska Curie Grant agreement No.722651 (SEPOMO). The Région Pays de la Loire is acknowledged for the grant of C. D. (Projet étoile montante SAMOA). Benjamin Siegler is thanked for his help on structure solving by NMR experiments. LAG thanks Agence Nationale de la Recherche (SADAM ANR-16-CE07-0015-02) for her grant. S.L. and C.R. thank the Office of Naval Research Young Investigator Program (award no. N00014-18-1-2448) for their support of this project. Supercomputing resources on the Lipscomb High Performance Computing Cluster were provided by the University of Kentucky Information Technology Department and the Center for Computational Sciences (CCS).

## Notes and references

$^{\dagger}$ These authors contributed equally.

- (1) (a) Feng, J.; Jiang, W.; Wang, Z. *Chemistry – An Asian Journal* **2018**, *13*, 20(b) Sun, M.; Müllen, K.; Yin, M. *Chemical Society Reviews* **2016**, *45*, 1513.
- (2) (a) Grayshan, P. H.; Kadhim, A. M.; Perters, A. T. *Journal of Heterocyclic Chemistry* **1974**, *11*, 33(b) Qian, X.; Mao, P.; Yao, W.; Guo, X. *Tetrahedron Letters* **2002**, *43*, 2995(c) Danko, M.; Hrdlovič, P.; Chmela, Š. *Polymer Degradation and Stability* **2011**, *96*, 1955.
- (3) (a) Josse, P.; Li, S.; Dayneko, S.; Joly, D.; Labrunie, A.; Dabos-Seignon, S.; Allain, M.; Siegler, B.; Demadrille, R.; Welch, G. C.; Risko, C.; Blanchard, P.; Cabanetos, C. *Journal of Materials Chemistry C* **2018**, *6*, 761(b) Payne, A.-J.; Rice, N. A.; McAfee, S. M.; Li, S.; Josse, P.; Cabanetos, C.; Risko, C.; Lessard, B. H.; Welch, G. C. *ACS Applied Energy Materials* **2018**, *1*, 4906(c) Dayneko, S.

## PAPER

New Journal of Chemistry

- V.; Hendsbee, A. D.; Cann, J. R.; Cabanetos, C.; Welch, G. C. *New Journal of Chemistry* **2019**, *43*, 10442.
- (4) Kollár, J.; Chmela, Š.; Hrdlovič, P. *Journal of Photochemistry and Photobiology A: Chemistry* **2013**, *270*, 28.
- (5) (a) Turro, N. J.; Ramamurthy, V.; Scaiano, J. C. *Photochemistry and Photobiology* **2012**, *88*, 1033(b) Penfold, T. J.; Gindensperger, E.; Daniel, C.; Marian, C. M. *Chemical Reviews* **2018**, *118*, 6975(c) Zobel, J. P.; Nogueira, J. J.; González, L. *Chemistry – A European Journal* **2018**, *24*, 5379.
- (6) (a) Schmidt, R.; Tanielian, C.; Dunsbach, R.; Wolff, C. *Journal of Photochemistry and Photobiology A: Chemistry* **1994**, *79*, 11(b) Zhang, L.; Huang, Z.; Dai, D.; Xiao, Y.; Lei, K.; Tan, S.; Cheng, J.; Xu, Y.; Liu, J.; Qian, X. *Organic Letters* **2016**, *18*, 5664.
- (7) Shie, J.-J.; Liu, Y.-C.; Lee, Y.-M.; Lim, C.; Fang, J.-M.; Wong, C.-H. *Journal of the American Chemical Society* **2014**, *136*, 9953.
- (8) (a) Plaza-Medina, E. F.; Rodríguez-Córdoba, W.; Morales-Cueto, R.; Peon, J. *The Journal of Physical Chemistry A* **2011**, *115*, 577(b) Crespo-Hernández, C. E.; Burdzinski, G.; Arce, R. *The Journal of Physical Chemistry A* **2008**, *112*, 6313(c) Vogt, R. A.; Reichardt, C.; Crespo-Hernández, C. E. *The Journal of Physical Chemistry A* **2013**, *117*, 6580.
- (9) Galland, M.; Le Bahers, T.; Banyasz, A.; Lascoux, N.; Duperray, A.; Grichine, A.; Tripier, R.; Guyot, Y.; Maynadier, M.; Nguyen, C.; Gary-Bobo, M.; Andraud, C.; Monnereau, C.; Maury, O. *Chemistry – A European Journal* **2019**, *25*, 9026.

# Nitration of the benzothioxanthene: towards a new class of dyes with versatile photophysical properties

José María Andrés Castán,<sup>†‡</sup> Laura Abad Galán,<sup>‡</sup> Shi Li,<sup>‡</sup> Clément Dalinot,<sup>†</sup> Pablo Simón Marqués,<sup>†</sup> Magali Allain,<sup>†</sup> Chad Risko,<sup>‡\*</sup> Cyrille Monnereau,<sup>‡</sup> Olivier Maury,<sup>‡\*</sup> Philippe Blanchard,<sup>†</sup> Clément Cabanetos<sup>†\*</sup>

<sup>†</sup>CNRS UMR 6200, MOLTECH-Anjou, University of Angers, 2 Bd Lavoisier, 49045 Angers, France

<sup>‡</sup>Department of Chemistry & Center for Applied Energy Research, University of Kentucky, Lexington, KY 40506, USA

<sup>\*</sup>Univ Lyon, ENS de Lyon, CNRS UMR 5182, Université Claude Bernard Lyon 1, F-69342 Lyon, France.

